Face Authentication Using Thermal Imaging

S. Athira[✉] and O. V. Ramana Murthy

Department of Electrical and Electronics Engineering, Amrita School of
Engineering, Coimbatore, Amrita Vishwa Vidyapeetham, Coimbatore, India
athirasasdhar@gmail.com

Abstract. The objective of the paper is to develop an algorithm for face
authentication using thermal imaging. Thermal imaging makes use of thermal
cameras to detect infrared radiation emitted by objects. Thermal images are
especially useful for face detection and authentication because of its low sen-
sitivity to illumination changes and its ability in detecting disguises. The
objective of the project is achieved through three stages. In the first stage, an
existing algorithm is verified by implementing it on the benchmark dataset.
Currently existing face authentication algorithms have only been verified by
implementing on datasets having plain background i.e. images without any
background objects. There is a need to investigate the efficiency of face
authentication algorithms on realistic scenarios. So, in the second stage an effort
had been put forth to create a new dataset of images with realistic background
and analyse the performance of various existing face authentication algorithms
on the new dataset.

Keywords: Face authentication · Thermal imaging · Dataset extension

1 Introduction

Identification systems has a lot of applications spanning from governmental projects
like border control or criminal identification to civil purposes like e-commerce, net-
work access or transport. Out of the existing identification systems, biometrics has
become very popular. It is the most reliable identification system since it depends upon
the physiological characteristics of a person which is unique for every person in this
planet and cannot be stolen or swapped. Different physiological features can be used as
biometrics such as iris, retina, face etc.

Face authentication is one of the most popular biometric identification systems. It is
more direct, user-friendly and convenient compared to other methods. There are many
existing face authentication systems in visible spectrum. But such systems may fail
when there is a variation in illumination. Further, such systems can be easily spoofed
by using disguises or by using photographs. Such systems cannot distinguish a live face
from a non-live face. A secure system needs liveness detection to guard against such
spoofing.

These challenges can be met with the help of thermal imaging. Thermal imaging makes use of thermal cameras to detect infrared radiation emitted by objects. Since thermal imaging depends on the heat emitted there is no issue of illumination variation. Only a live face will emit thermal radiation. So liveness detection can be easily carried out with thermal imaging. Also the radiation emitted by human face is at a different range compared to other objects thus aiding in detecting disguises.

Previous works done by researchers indicate that many face authentication algorithms such as Principal Component Analysis (PCA) [1], Local Binary Pattern (LBP), Histogram of Oriented Gradients (HOG) etc. which gives very accuracy in face authentication in visible spectrum works very well in the case of thermal images too. However, they were all verified on datasets containing non-realistic backgrounds. There are no other background objects. But that may not always be the case. There may be other objects with similar spectral range in the background. The work presented here analyses the performance of various face authentication algorithms on a newly created database with images having realistic background.

The paper is organized as follows: Sect. 2 provides an overview on related work done previously by other authors. Section 3 explains the method implemented to achieve the objective. Section 4 presents the results obtained. Section 5 gives the conclusion reached and future scope of the work.

2   Literature Survey

Researchers have realized the potential of thermal imaging in the area of human identification. One of the earliest works on the topic was conducted by Chen et al. He had conducted some significant studies on face authentication in visible and infrared spectrum using principal component analysis (PCA) and has presented the results in [2]. The algorithm was implemented on their dataset called C-X1. Database consists of 10,916 images in both visible and IR spectrum from 488 subjects.

Guzman et al. [3] proposed an algorithm that does face authentication based on the vasculature information which is different for every person. The algorithm is implemented by using localization of active contours and morphological operations. The features are then matched using similarity measurements. The proposed algorithm was implemented on C-X1 dataset and on a newly created dataset comprising 13 subjects. When implemented on the Guzman dataset it gave an average recognition rate of 89% and a recognition rate of 68.5% on C-X1 dataset by using different similarity measures. The poor performance of algorithm on C-X1 dataset was claimed to be due to the lack of non uniformity correction in the dataset. Major drawback is that the algorithm was validated only on a small dataset.

Carrapico et al. [4] has taken into consideration several image descriptors and analyzed their performance in face authentication using thermal images. The image descriptors considered include Gabor Bank-Filters, Localized Binary Patterns (LBP), Colour and Edge Directivity Descriptor (CEDD) [5] and Fuzzy Colour and Texture Histogram (FCTH) [6]. The four algorithms were implemented on dataset provided by University of Science and Technology, China along with a k-nn classifier. Out of the four the Localized Binary Patterns (LBP) feature descriptor gave the highest accuracy of 91%.

Xie and Wang [7] has proposed a modified LBP based feature extraction algorithm for face authentication using thermal imaging. The major drawback of LBP is its large dimensionality. The proposed approach tackles this problem by selecting personalized features for each subject. The algorithm was implemented on their own dataset of 400 thermal images of 40 subjects in combination with KNN classifier. Its performance was compared with other LBP based techniques. Their algorithm gave the recognition rate of 98.2%.

Espinosa-Duró et al. [8] created a database of thermal face images. It consist of 41 subjects (32 males and 9 females). Visible and thermal images of all the subjects were captured under three different illumination conditions: IR (infrared illumination), AR (artificial illumination) and NA (Natural illumination). A feature extraction method based on discrete cosine transform (DCT) was implemented.

In all the above mentioned works the feature extraction algorithms were verified only on datasets containing images with plain background. However these algorithms need to be verified on images with realistic background as well.

3   Methodology

Figure 1 depicts the basic flow diagram of the face authentication process.
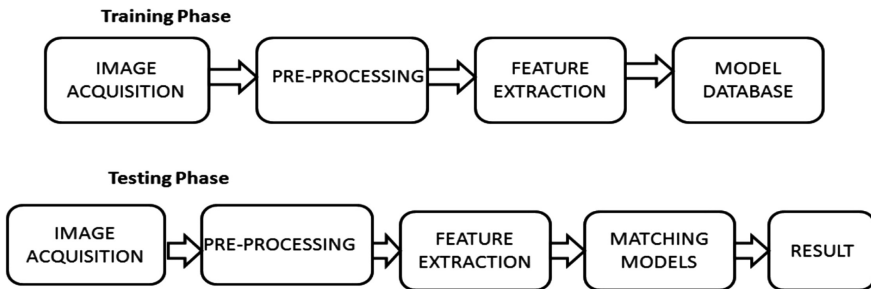

Fig. 1   Block diagram

(a) *Pre-Processing*: A median filter with a kernel size of 5 was used to remove the higher frequencies and the impulse noises while preserving the edges.
(b) *Feature Extraction*: Four different feature extraction algorithms were implemented on the two datasets: Local Binary Pattern (LBP), Histogram of Oriented Gradients (HOG), Pyramid Histogram of Oriented Gradients (PHOG) and Discrete Cosine Transform (DCT).

- **Local Binary Pattern (LBP)** [7]: It is a powerful feature for texture classification. It has two major parameters: P and R. P is the number of neighboring pixels and R is the radius. Here P is taken as 8 and R as 1. The entire image is divided into non-overlapping blocks of uniform size of 16×16 pixels. For each pixel in the block, its intensity is compared with 8 neighboring pixels at a radius of 1 pixel. A binary code for centre pixel

$$LBP_{P,R}(g_c) = \sum_{i=0}^{P-1} 2^i \cdot B \tag{1}$$

is generated based on the comparison as per the following equation:

$$B = \begin{cases} 1, & g_i - g_c > 0 \\ 0, & g_i - g_c < 0 \end{cases} \tag{2}$$

where g_c is the gray value of the central pixel, g_i is the gray value of the neighboring pixels. $g_i - g_c$ is the generated binary code for central pixel g_c. A binary value of 1 is assigned if the gray value of central pixel is less than that of the neighboring pixels and a value of 0 is assigned if the gray value of central pixel is greater than that of the neighboring pixels. The number bits depend on P value. Since it is taken as 8 here an 8 bit binary code is generated for each pixel.

For each non-overlapping block histogram is computed based on the following equations:

$$H(r) = \sum_{x_c}^{M-1} \sum_{y_c}^{N-1} f\left(LBP_{P,R}(x, y), r\right) \tag{3}$$

$$f\left(LBP_{P,R}(x, y), r\right) = \begin{cases} 1 & LBP_{P,R}(x, y) = r \\ 0 & otherwise \end{cases} \tag{4}$$

The final feature matrix is formed by concatenating normalized histogram of the binary patterns of all the blocks in the image.

- **Histogram Of Oriented Gradients (HOG)** [9]: It is a scale invariant feature descriptor. Entire image is divided into uniform blocks with 50% overlapping. The gradient of an image is defined by:

$$\Delta f = \begin{pmatrix} g_x \\ g_y \end{pmatrix} = \begin{pmatrix} \frac{\partial f}{\partial x} \\ \frac{\partial f}{\partial y} \end{pmatrix} \tag{5}$$

where $\frac{\partial f}{\partial x}$ is the gradient in x direction and $\frac{\partial f}{\partial y}$ is the gradient in y direction.

The gradient direction is calculated by:

$$\theta = \tan^{-1}\left(\frac{g_y}{g_x}\right) \tag{6}$$

The gradient magnitude and direction is calculated for each pixel in each block. Then a histogram of gradients is computed for each cell (9 bins, 0°–360°. Concatenating the normalized histograms all the blocks forms the final feature vector.

- **Pyramid Histogram of Oriented Gradients** [10]: It is a variant of HOG. HOG features are calculated for three different block sizes. Then final feature vector is formed by concatenating the normalized histograms of all the levels.
- **Discrete Cosine Transform** [8]: It is an invertible linear transform. The image is converted into frequency domain by applying DCT. DCT2 defined by the following equation is used:

$$X[k,l] = \frac{2}{N} \cdot c_k \cdot c_l \cdot \sum_{m=0}^{a-1} \sum_{n=0}^{b-1} x[m,n] \cos\left(\frac{(2n+1)l\pi}{2N}\right)$$

where a and b indicate the number of coefficients in x and y direction, N is the total number of significant coefficients and c_k and c_l are defined as:

$$c_k, c_l = \begin{cases} \frac{1}{\sqrt{2}} \, to \, k = 0, \, l = 0 \\ 1 \, to \, k = 1, 2, \ldots a-1 \quad and \quad l = 1, 2, \ldots b-1 \end{cases}$$

The DCT coefficients indicate the importance of frequencies in it. The first coefficient signifies the lowest frequency component and carries the most significant information. Higher frequencies are mostly noise components. The first N DCT coefficients are used as feature vector.

(c) *Classification*: The features formed were classified using two popular classifiers: K-Nearest Neighbours (KNN) [11] and Support Vector Machine (SVM) [12].

A k-fold cross validation process was carried out to get the classification accuracy. Here k was chosen as 10. The entire dataset is divided into 10 random groups. Each group is taken as the test matrix and the remaining group as training groups in an iterative process. The classification accuracy is calculated as follows:

$$A = \frac{C}{T}$$

where A is the classification accuracy, C is the number of correct classifications and T is the total number of classifications.

(d) *Datasets*: The algorithm was implemented on two datasets: the publicly available Carl database and a newly created database. Carl database consists of thermal, visible and infrared images of 41 subjects (32 males and 9 females) under three different illumination conditions: natural illumination, artificial illumination and infrared illumination. The dataset also contains face localized images of the same. There are many face localization algorithms in existence like level set algorithm [13] etc. The face localized images in Carl database were created using a new algorithm [14] (Figs. 2, 3 and 4).
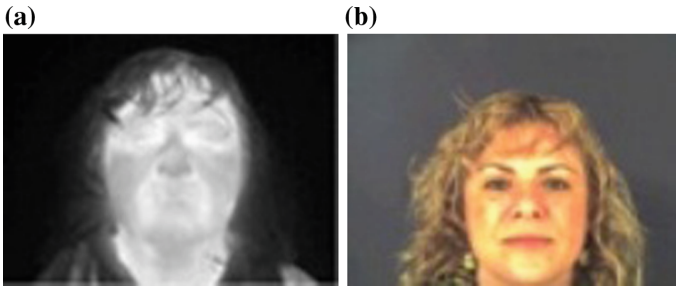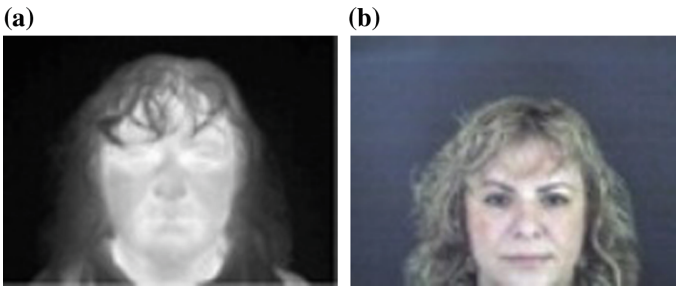
(a)   **(b)**

Fig. 2 a Thermal, **b** Visible

(a)   **(b)**

Fig. 3 a Thermal, **b** Visible
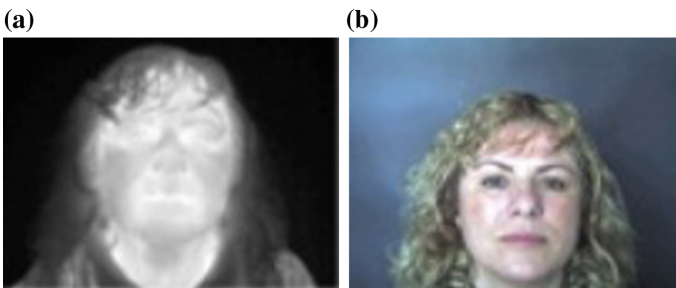
(a)   **(b)**

Fig. 4 a Thermal, **b** Visible

The newly created database consists of thermal and near infrared images of 30 subjects (10 males and 20 females) with realistic backgrounds. The backgrounds vary for different subjects. The images were captured at different times of the day from morning 9 a.m to evening 4 p.m to take into account the temperature variations that occur. The thermal images were acquired using FLIR One thermal camera with a temperature range of −20° to 120 °C and thermal sensitivity of 0.1 °C. The images captured are in jpg format with dimensions of 480 × 640 pixels. The near infrared

images were captured using a MAPIR NDVI + Red Survey 2 camera with a spectral range of 700 nm–1 mm (Fig. 5).

The captured images were 3 dimensional with the infrared component as the 2nd dimension. So only that was extracted from all the images. The images are in raw jpg format with dimensions of 3840 × 2160 pixels. The images were acquired with an approximate distance of 1 m between the subject and the camera. Unlike the existing thermal face databases, the images were captured with a non-plain realistic background.
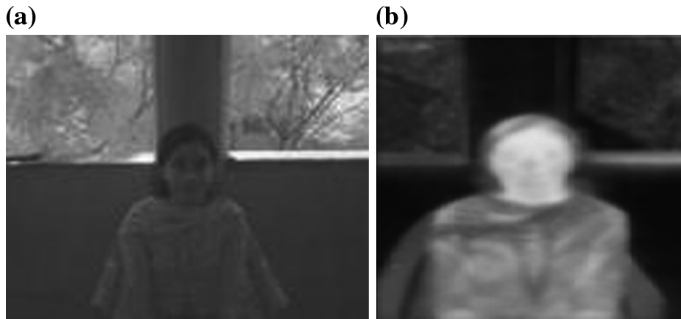
(a)   **(b)**

Fig. 5 **a** Near infrared, **b** Thermal

4 Results

The results obtained are presented in Tables 1, 2 and 3.

Table 1 Classification accuracy using Carl and new database

Algorithm	Carl—KNN (%)	Carl—SVM (%)	New—KNN (%)	New—SVM (%)
LBP	41	15	30	10
HOG	38	35	28	25
PHOG	30	25	23	20
DCT	37	56.2	29	45

Table 1 depicts the classification accuracy for KNN and SVM on the different feature extraction algorithms. The tables indicate that the accuracy is highest for LBP features. Also, it is observed that the accuracy value decreases when considering images with non-plain background.

Table 2 Classification accuracy of face localized images

Algorithm	KNN (%)	SVM (%)
LBP	91	88
HOG	90.5	88
PHOG	89	25
DCT	81.7	87.8

Table 2 gives the accuracies when the algorithms were implemented on the face localized images of Carl database. The results indicate the advantage of face localizing the images before feature extraction.

Table 3 Comparison of different illuminations using KNN

Algorithm	NA (%)	AR (%)	IR (%)
LBP	94.5	91	90.7
HOG	91	90.5	91
PHOG	88	89	90
DCT	98	97	98

Table 3 compares the accuracy values for different illuminations. It can be observed that the accuracy does not vary much with change in illumination.

5   Conclusion and Future Work

A new dataset of thermal and near infrared face images with non-plain realistic backgrounds was created. Different feature extraction algorithms (LBP, HOG, PHOG, DCT) were compared by implementing them on a benchmark dataset and on a newly created dataset. The LBP features gave the highest accuracy. Also, the accuracy decreased significantly when implemented on the new dataset because of its non-plain background. Also, accuracy increased dramatically when face localization was done before feature extraction. There was not much change in accuracy when implemented for different illuminations conforming that thermal images remain unaffected by illumination variations.

Face localization algorithm for images with plain background already exists. Such algorithms for non-plain backgrounds should be investigated. The algorithm needs to be verified on a larger dataset.

References

1. Nimmy, K., Sethumadhavan, M.: Biometric authentication via facial recognition (2014)
2. Chen, X., Flynn, P.J., Bowyer, K.W.: Ir and visible light face recognition. Comput. Vis. Image Underst. **99**(3), 332–358 (2005)
3. Guzman, A.M., Goryawala, M., Wang, J., Barreto, A., Andrian, J., Rishe, N., et al.: Thermal imaging as a biometrics approach to facial signature authentication. IEEE J. Biomed. Health Inform. **17**(1), 214–222 (2013)
4. Carrapico, R., Mourão, A., Magalhaes, J., Cavaco, S.: A comparison of thermal image descriptors for face analysis. In: 2015 23rd European Signal Processing Conference (EUSIPCO). IEEE, pp. 829–833 (2015)
5. Chatzichristofis, S., Boutalis, Y.: Cedd: color and edge directivity descriptor: a compact descriptor for image indexing and retrieval. In: *Computer Vision Systems*, pp. 312–322 (2008)

6. Chatzichristofis, S.A., Boutalis, Y.S.: Fcth: Fuzzy color and texture histogram—a low level feature for accurate image retrieval. In: Ninth International Workshop on Image Analysis for Multimedia Interactive Services, 2008. WIAMIS'08. IEEE, pp. 191–196 (2008)

7. Xie, Z., Wang, Z.: Infrared face recognition based on personalized features selection of lbp. In: 2015 7th International Conference on Intelligent Human-Machine Systems and Cybernetics (IHMSC), vol. 2. IEEE, pp. 228–231 (2015)

8. Espinosa-Duró, V., Faundez-Zanuy, M., Mekyska, J.: A new face database simultaneously acquired in visible, near-infrared and thermal spectrums. Cogn. Comput. **5**(1):119–135 (2013)

9. Dalal, N., Triggs, B.: Histograms of oriented gradients for human detection. In: IEEE Computer Society Conference on Computer Vision and Pattern Recognition, 2005. CVPR 2005, vol. 1. IEEE, pp. 886–893 (2005)

10. Bai, Y., Guo, L., Jin, L., Huang, Q.: A novel feature extraction method using pyramid histogram of orientation gradients for smile recognition. In: 2009 16th IEEE International Conference on Image Processing (ICIP). IEEE, pp. 3305–3308 (2009)

11. Ameur, B., Masmoudi, S., Derbel, A.G., Hamida, A.B.: Fusing gabor and lbp feature sets for knn and src-based face recognition. In: 2016 2nd International Conference on Advanced Technologies for Signal and Image Processing (ATSIP). IEEE, pp. 453–458 (2016)

12. Suykens, J.A.., Vandewalle, J.: Least squares support vector machine classifiers. Neural Process. Lett. **9**(3), 293–300 (1999)

13. Kumaravel, M.S Karthik, P.S., Soman, K.: Human face image segmentation using level set methodology. Int. J. Comput. Appl. **44**(12), 16–22 (2012)

14. Marzec, M., Koprowski, R.: Wróbel, Z., Kleszcz, A., Wilczyński, S.: Automatic method for detection of characteristic areas in thermal face images. Multimedia Tools Appl. **74**(12), 4351–4368 (2015)